Analytical Study of Permanent Magnet Cylindrical Synchronous Machines fed by Rectangular or Sinusoidal Currents

André YOUMSSI [2, 1], Abderrezack REZZOUG [2], François Michel SARGOS [2].

[1]. University of Ngaoundéré, IUT- ENSAI, P.O.Box 454 Ngaoundéré -Cameroon- Fax : (237) 25.27.67

[2]. GREEN-INPL, 02 Avenue de la Forêt de Haye 54516 Vandoeuvre-Les-Nancy Cedex -France-

ABSTRACT

This paper deals with an important problem : the analytical study of some Permanent Magnets Machines fed by current inverters. The final aim the authors are looking for consists of showing that such analytical study can be handled and could be used for instance in the pre-dimensioning and the optimization of those machines. The originality of the methodology is based on the development of original suitable models of new permanent magnets, and on some eccentric specific analytical approaches of potentials, field and torque calculations in permanent magnets cylindrical synchronous motors. Under some simplifying assumptions, the analytical methods are very convenient for machine designing. The present study involves two methods, the first one based on the separation of variables in Laplace's equation and the second one on magnetic images. One of the results compared with those of a numerical finite difference program show a close agreement. The effect of both radial and azimuth magnetizations is considered. The analysis is then applied to a synchronous machine fed by rectangular or sinusoidal current waves.

PACS : 84.50+d Electric Motors - 85.70.-w Magnetic Devices

RESUME

Cet article traite d'un important problème scientifique et technique de notre époque : Les études analytiques de quelques structures de Moteurs à Aimants Permanents alimentés par des onduleurs de courants. L'objectif principal visé par les auteurs consiste à montrer que de telles analyses peuvent actuellement être développées et utilisées par exemple dans les études de pré-dimensionnement, et d'optimisation de tels moteurs. L'originalité de la méthodologie est basée sur une modélisation originale et adéquate des aimants permanents, et sur d'originales et spécifiques approches analytiques des potentiels scalaires, des potentiels vecteurs, des champs magnétiques, et du couple, dans les structures cylindriques des moteurs synchrones à aimants permanents surfaciques. Les méthodes analytiques conviennent au mieux, moyennant quelques hypothèses simplificatrices, à la conception des moteurs électromécaniques. La présente étude met en oeuvre deux méthodes : La première est basée sur la séparation des variables dans la résolution de l'équation de Laplace dans des milieux cylindriques, et la deuxième sur une judicieuse et non moins originale application de la méthode des images magnétiques aux calculs analytiques des moteurs à aimants permanents. Quelques uns des résultats comparés à ceux obtenus par le biais d'un code numérique utilisant la méthode des différences finies, montre de réels similitudes. Quelques effets, tels ceux de la présence ou non des aimants radiaux, et/ou azimutaux sont observés. L'étude est ensuite appliquée à l'analyse d'un moteur synchrone alimenté par des onduleurs de courants rectangulaires ou sinusoïdaux..

List of Principal Symbols:

This list of principal symbols should help the explanation of all equations written in the text, and thus make the reading of the paper very easy.

Ajq : intermediate variable in the calculus of the total torque G.
an: coefficient of harmonic number n in K(Ro, q) series expansions.
A: amplitude of the only existing (with respect to z-axis) component of the vector potential.
A1: amplitude of the only existing (with respect to z-axis) component of the vector potential in region 1.
A2: amplitude of the only existing (with respect to z-axis) component of the vector potential in region 2.
Ak: amplitude of the only existing (with respect to z-axis) component of the vector potential in region 2 due to kth current image surface source .
: the vector potential
: the magnetic flux density vector
BN, Br(q); Br(r,q) : radial component of the magnetic flux density vector.
BN2, Br2(r,q): radial component of the magnetic flux density vector in region 2.
BT2, Bq2(r,q): tangential component of the magnetic flux density vector in region 2.
Br(T): radial component of the magnetic flux density vector, in tesla.
bn: coefficient of harmonic number n in s *(Ro, q) series expansions.
b : coefficient in the expansion of 1/d
bn; b'n: a factor in the calculation of I, J, and J'
cn: coefficient of term (r/Ro)n in V1* series expansions.
dn: coefficient of term (Ro /r)n in V1* series expansions.
d: distance from the axis of a cylinder with R radius, to a given infinite line of charges or of current
D: distance from the axis of a cylinder with R radius, to the magnetic image of a given infinite line of charges or of current
fn: coefficient of term (r/Ro)n in V2* series expansions.
gn: coefficient of term (Ro /r)n in V2* series expansions.
HN : radial component of the magnetic field vector.
HN2: radial component of the magnetic field vector in region 2.
HT : tangential component of the magnetic field vector.
HT2: tangential component of the magnetic field vector in region 2.
iq(t) current in phase q
I: intermediate variable approximated by Tchebychev's polynomials and used in the calculation of Vk*
j : variable representing the rang of an harmonic in Fourier's series : volume current density vector in Ampere's model representation of a magnetized volume
J*: current density of a given infinite line
J; J': intermediate variables approximated by Tchebychev's polynomials and used in the calculation of Ak
Ks(q, t): equivalent current density developed into Fourier's series
Ks0 : a constant multiplying the amplitude of the equivalent

Contact Persons: Dr André YOUMSSI
The University of NGAOUNDERE - I.U.T - E.N.S.A.I.
P.O.Box 454 NGAOUNDERE - Fax : 25.27.67
Satellite Fax : 00 871 761 330 643 - CAMEROON

current density Ks(q, t)
Kj: amplitude of j harmonic in Fourier's series development of the equivalent
Current density Ks(q, t) : surface current density vector in Ampere's model representation of a magnetized volume
K(Ro, q): current density on surface Ro in Coulomb's model representation of azimuth magnets
Ko: amplitude of the fundamental rank of K(Ro, q).
K(Ri, q): current density on surface Ri in Coulomb's model representation of azimuth Magnets
lm : half length of the magnets in three dimensions view
Lm : half length of the motor in three dimensions view
m : number of electric phases
: magnetization vector in a given volume
nd: angular density of phase conductors
n: rank of Fourier's series
: exterior unit vector in Ampere's model or Coulomb's model representation of a magnetized volume
p: number of poles-pair.
q : variable representing an electric phase
r: position of the studied point in polar coordinates.
R: radius of a given magnetic cylinder
Rs: inner radius of the stator.
Ri: inner radius of the magnets.
Ro: outer radius of the magnets.
rk: positions of the infinity of magnetic images inside the rotor (rk < Ri) for original sources on Ro.
Rk: positions of the infinity of magnetic images inside the stator (Rk > Rs) for original sources on Ro.
r'k: positions of the infinity of magnetic images inside the rotor (rk < Ri) for original sources on Ri.
R'k: positions of the infinity of magnetic images inside the stator (Rk > Rs) for original sources on Ri.
Sa: intermediate variable used in the calculation of coefficients gn, dn, an, and bn.
Sb: intermediate variable used in the calculation of coefficients fn, gn, cn, and dn.
t: variable representing the time
V*: the magnetic scalar potential.
V* (T m): the magnetic scalar potential in Tesla - meter.
V1*: the magnetic scalar potential in region 1.
V2*: the magnetic scalar potential in region 2.
Vk*: the magnetic scalar potential in region 2 due to kth charge image surface source .
q0: phase angular step.
G: total torque.
q: variable in polar co-ordinates representing a geometric angle
q (°): variable in polar co-ordinates representing a geometric angle, in degree
qra: half aperture of a one pole radial permanent magnet
qaz: half aperture of a one pole azimuth permanent magnet
qis: gap angle between radial and azimuth permanent magnets in the same pole
s *: surface charge density in Coulomb's model representation of a magnetized volume
s *(Ro, q): charge density on surface Ro in Coulomb's model representation of radial magnets
s *(Ri, q): charge density on surface Ri in Coulomb's model representation of radial magnets
so*: amplitude of the fundamental rank of s*.
n: rank of the harmonics in Fourier's series.
r *: volume charge density in Coulomb's model representation of a magnetized volume
mo: magnetic permeability of free space.
an: coefficient of term (r/Ro)n in A1 series expansions.
bn: coefficient of term (Ro /r)n in A1 series expansions.
gn: coefficient of term (r/Ro)n in A2 series expansions.
dn: coefficient of term (Ro /r)n in A2 series expansions.
l*: charge density of a given infinite line
r : intermediate variable used in the calculation of the positions of magnetic images
j: variable used in the calculation of I, J, and J'
Y: dummy variable used in the calculation of I, J, and J'
Yi: ith point of Tchebychev's interpolation
: index used in the interpolation of 1/d
: maximum number of points in the Tchebychev's interpolation
bn: a factor in the calculation of Vk* , Ak and Br2(r,q)
b'n: a factor in the calculation of Ak and Br2(r,q).

Introduction

The increasing need of high performance machines able to develop, for instance, great mass torques at low speed or important mass powers at high speed, leads to use efficient materials like permanent magnets [1].

Modern rare earth magnets have great coercive force (H_c), great remnant magnetization (B_r), and so can be employed in high performance low weight machines. They allow large magnetic air gaps without significant reduction of global efficiency [2]. Ferrite magnets are suitable for low cost machines but with lower volume performances [3].

These machines can be classified either from their external geometry : long, short, and flat motors, or from the rotor shape and the disposition of magnets : without polar pieces, with polar pieces, with or without flux concentration [5, 8].

The machines studied here have sector shaped permanent magnets with radial and (or) azimuth magnetization without polar pieces. Under some assumptions the analytical methods are specially suitable to such structures. The proposed methods for the calculations are two dimensional and are based on :

- the separation of variables of Laplace's equation in cylindrical domains. Both vector and scalar potentials are considered.
- the application of magnetic images.

The results are compared with those obtained owing to a numerical method : F.D.M. (Finite Differences Method) and discussed. They are then applied to a synchronous machine fed by either sinusoidal or rectangular current waves.

1.ORIGINAL MODELIZATION OF THE STUDIED MOTORS AND EXPRESSION OF THE TORQUE

2.1.Some Hypothesis and the studied motors modelizations.

We assume that :
- the rotor and the stator have infinite permeability,
- the system can mainly be considered as two-dimensional
- the magnetic gap is large enough to neglect the armature reaction,
- the real armature currents are classically replaced by their equivalent current densities,
- the magnets are permanent and have linear demagnetization characteristics,
- eddy currents are not considered.

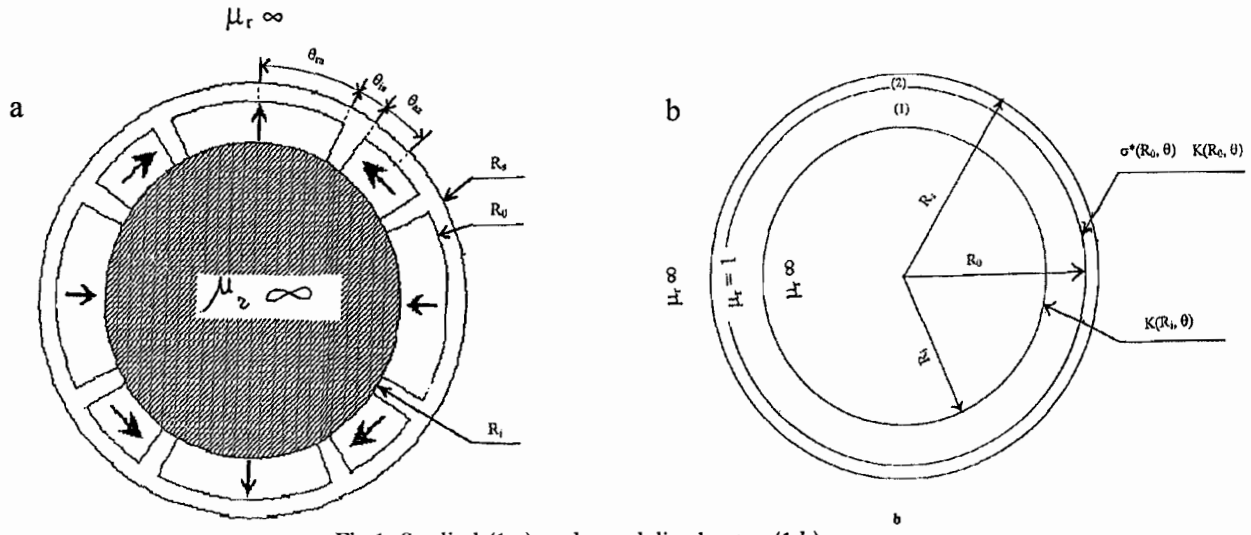

Fig.1 Studied (1.a) and modelized rotor (1.b).

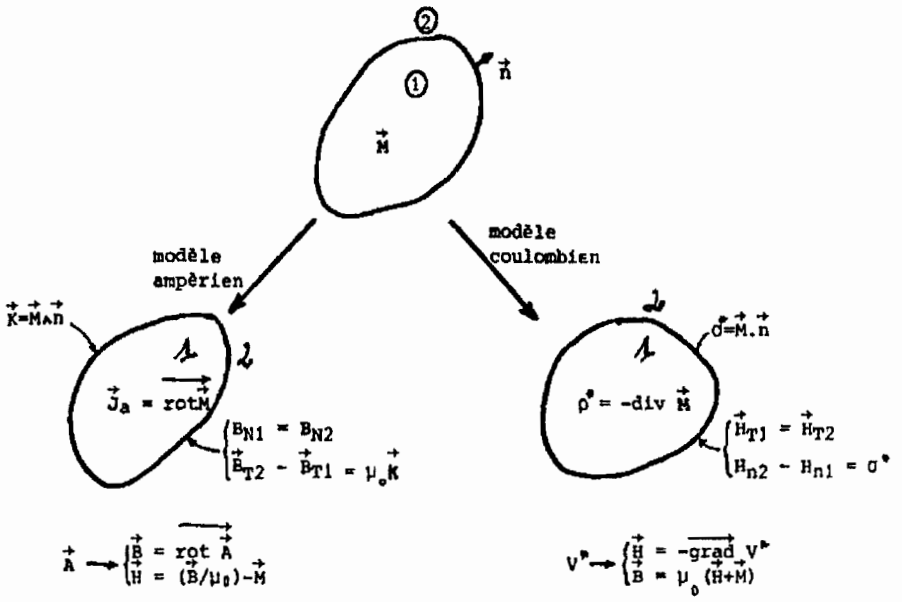

Fig.2.a
The two possible models of a magnetized volume.

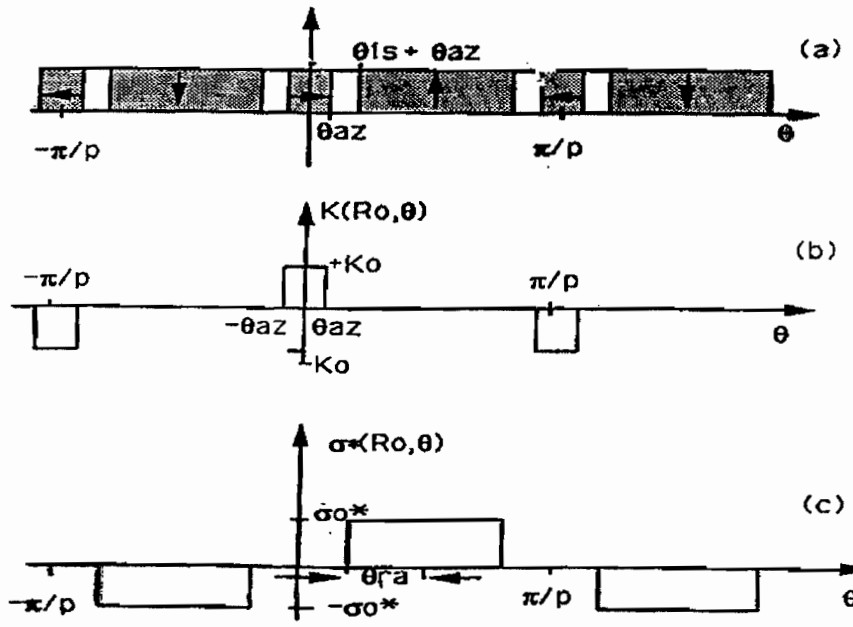

Fig.2.b
a) Developed geometry of the rotor.
b) Equivalent current densities.
c) Equivalent charge densities.

2.2. EXPRESSIONS OF THE TORQUE

Considering a machine with 2p poles and m phases, two cases can be distinguished according to the angular density n_d of phase conductors. This angular density can be constant or not.

2.2.1. The case of constant angular density of phase conductors n_d

The density of phase conductors can be considered as constant over a phase angular step $\theta_o = \pi/p$ m. This case includes slot less machines and also slotted machines with one-layer slots under some approximations. In such conditions the total torque Γ is the sum of all torques per phase, each of them being calculated independently. Γ can then be written as follows :

$$\Gamma = 2\, p\, R_s n_d \sum_{q=1}^{m} i_q(t) \int_{\theta_o} B_r(\theta) d\theta \qquad (1)$$

where R_s is the radius of the stator, B_r the radial component of the flux density, and iq the current in phase q.

2.2.2. The case of none constant angular density of phase conductors n_d

In the general case, the density of conductors n_d cannot be considered as constant and the fundamental variable becomes the equivalent current density K_s developed owing to the distribution theory, into Fourier's series as follows.

$$K_s(\theta,t) = K_{so}\, i_q(t) \sum_{j=o}^{\infty} K_j \cos j\left[\theta - \frac{2\pi(q-1)}{m}\right] \qquad (2)$$

The expression of the total torque is now :

$$\Gamma = 2\, p\, R_s K_{so} \sum_{q=1}^{m} \sum_{j=o}^{\infty} K_j i_q(t)\, A_{jq} \qquad (3)$$

with :

$$A_{jq} = \int_{\theta_o} B_r(\theta) \cos j\left[\theta - \frac{2\pi(q-1)}{m}\right] d\theta \qquad (4)$$

Expression (1) is simpler to use for independent phases (brush less DC motors, auto-synchronous motors), while expression (2) is suitable for poly-phase machines with distributed windings. In either case, only the radial component of the flux density has to be known in the calculation of Γ. For that, we should solve the Maxwell's equations in the air gap of the motors. The solutions of those equations are easily found out when the models of the sources, here the permanent magnets, are known. So let look for the mathematic models of those magnets, and then calculate B_r.

2.3. ORIGINAL MODELS OF SURFACE MAGNETS WITH RADIAL AND AZIMUTH MAGNETIZATIONS

The considered rotor has surface magnets which have angular widths θ_{ra} for radial magnets, and θ_{az} for azimuth magnets (Fig.1a). Since the analysis can be done by separating the effects of both magnets, we can introduce an angle θ_{is} so that (Fig.2.b) :

$$\theta_{ra} + \theta_{az} + \theta_{is} = \frac{\pi}{2p} \qquad (5)$$

2.4. ORIGINAL MODELS OF THE PERMANENT MAGNETS

One of the originality of the methodology used in this paper, is the mathematic model of the magnets. For that aim, it is now known that a magnetized volume such as a magnet with magnetization $\vec{M}$ can be represented using Ampere's model or Coulomb's model (Fig.2.a). This radial and azimuth magnets of this study (Fig.1.a) can then be replaced

- either by a surface current density $\vec{K} = \vec{M} \times \vec{n}$ and a volume current density $\vec{J}_v = \vec{\nabla} \times \vec{M}$ (Ampere's model).

or by a surface charge density $\sigma^* = \vec{M} \cdot \vec{n}$ and a volume charge density $\rho^* = \vec{\nabla} \cdot \vec{M}$ (Coulomb's model).

With $\vec{n}$ an exterior unit vector to the magnetized volume.

In this study the magnets are permanent so $\vec{\nabla} \times \vec{M}$ is equals zero, and the radial magnets must be built such that the amplitude of the magnetization M(r) varies as a function of 1/r, so $\vec{\nabla} \cdot \vec{M}$ will also equal zero. The study will then be very easy if we adopt Coulomb's model for radial magnets and Ampere's model for azimuth ones. This allows to replace either king of magnets by only two concentric cylindrical surfaces as shown on figure 1.b. assuming that R_i and R_o are the inner and the outer radii of the magnets. The deduced forms of the sources K and σ^* allow to develop them into Fourier's series as follows (Fig.2.b). For more clarity, the deduced coefficients, the motor data and all others symbols used in the following equations have been explained in the list of principal symbols part :

$$\sigma^*(R_o,\theta) = \sigma_o^* \sum_{n=o}^{\infty} b_n \sin \nu\,\theta \tag{6}$$

$$K(R_o,\theta) = K_o \sum_{n=o}^{\infty} a_n \cos \nu\,\theta \tag{7}$$

$$K(R_i,\theta) = \left(-\frac{R_o}{R_i}\right) K(R_o,\theta) \tag{8}$$

$$\sigma^*(R_i,\theta) = \left(-\frac{R_o}{R_i}\right) \sigma^*(R_o,\theta) \tag{9}$$

with :

$$\nu = (2n + 1)p \tag{10}$$

$$a_n = \left[\frac{4p}{\nu\pi}\right] \sin\, \nu\theta_{az} \tag{11}$$

$$b_n = (-1)^n \left[\frac{4p}{\nu\pi}\right] \sin\, \nu\theta_{ra} \tag{12}$$

3. THE SOLVING OF MAXWELL'S EQUATIONS IN THE AIRGAP OF THE MOTOR

In this section, we calculate the flux density created by the magnets. We denote zone 1 the region between the two cylindrical borders of the magnets and zone 2 the one between the outer surface of the magnets and the inner surface of the stator. The hypothesis assumed in part 2.1 are also here taken into account, so we have to solve a magneto-static problem [10].

Radial magnets as well as azimuth magnets will both contribute separately in the expression of the flux density. Ampere's model of azimuth magnets leads to a problem where sources are current densities, while Coulomb's model of radial magnets gives a problem where sources are magnetic charge densities (Figs.2.a, 2.b). Equivalent charge densities will generate the magnetic scalar potential V^*, and the current densities will create the vector potential A.

Considering only the radial magnets, the global model of Maxwell leads to write in region 2, $\vec{\nabla} \cdot \vec{B} = 0$, $\vec{\nabla} \times \vec{H} = 0$ and $\vec{B} = \mu_o \vec{H}$. But in the magnets we will have $\vec{B} = \mu_o \vec{H} + \vec{M}$. Equations in region 2, and radial permanent magnets properties ($\vec{\nabla} \cdot \vec{M} = 0$), indicate that the magnetic field is not rotational, and enable to introduce a scalar function so-called magnetic scalar potential V^* given by the equation $\vec{H} = -\vec{\nabla} V^*$. So, the contribution of the radial magnets to the flux density will be written in region 2 $\vec{B} = -\mu_0 \vec{\nabla} V^*$ where the scalar potential V^* must be searched (Fig.2.a).

Assuming now azimuth magnets model alone, and given the general model of Maxwell, we are facing a problem that involves stationary currents, a now classic vector, the so-called vector potential $\vec{A}$ of a rotational but solenoid field, is usually introduced, and is given by the equation $\vec{B} = \vec{\nabla} \times \vec{A}$, with the condition of solenoid character, also called Coulomb's gauge $\vec{\nabla} \times \vec{A} = 0$. So the contribution of the azimuth magnets to the flux density in region 2 can written $\vec{B} = \vec{\nabla} \times \vec{A}$ where the vector potential $\vec{A}$ needs to be calculated (Fig.2.a).

We can now calculate the scalar potential V^* due to the equivalent charges, and in two dimensions, the only existing (axial) component of the vector potential A due to the current densities.

Hence,

$$\vec{B} = -\mu_0 \vec{\nabla} V^* + \vec{\nabla} \times \vec{A} \qquad (13)$$

We have shown that only equivalent charges generate V*. So, we can write

$\vec{\nabla} . \vec{B} = \vec{\nabla} . (-\mu_0 \vec{\nabla} V^*) = 0$. This last equation leads in region 2 to Laplace's equation $\nabla^2 V^* = 0$, which will be solved using the boundary conditions.

It has been also set that only azimuth magnets create the vector potential which can be calculated by writing $\vec{\nabla} \times \vec{B} = \vec{\nabla} \times (\vec{\nabla} \times \vec{A}) = 0$. This equation conducts, using the Coulomb's gauge, to Laplace's equation in region .2 $\nabla^2 \vec{A} = 0$ which will also in this case be solved using the boundary conditions.

We will describe here two analytical methods, the results of which could be compared.

3.1. ORIGINALITY OF THE PROPOSED METHODOLOGY USING PERMANENT MAGNETS PROPERTIES

In addition to the suitable mathematic models of the permanent magnets, with the specific choice of charge densities for radial magnets, and current densities for azimuth magnets, the other originality of the proposed methodology consists also of developing semi-analytical expressions of the flux density and of the torque that can be used for a pre-dimensioning of the motors, and for an optimization of such machines. Those two possibilities, the pre-dimensioning and the optimization of the motors can not be easy to handle without analytical expressions of magnetic scalar potential, vector potential, flux density, and torque. Others advantages of such a study do exist, for instance the possibility of observing the influence parameters, each independently or by combination of more than one.

In the looking for those expressions, we will solve Maxwell's equations in the air gap of the motors, by using an analytical method based on the classic variable separation method, and an interesting other way to employ the method of magnetic images. We will then compare one of the results to those obtained owing to a finite difference program.

3.1.1.Analytical expressions of potentials with respect to permanent magnets properties.

In the solving of Maxwell's equations to find out the magnetic scalar potential and the vector potential, cylindrical or polar coordinates are obviously the most suitable ones.

Let us consider only charges densities as sources. In the solving of Maxwell's equations when looking for the magnetic scalar potential, we have a problem where the potential is null on the interior face of the stator and on the rotor because both rotor and stator are supposed to present infinite magnetic permeability, while the interior of the radial magnets is empty space. The magnetic potential property of continuity and the jump of the radial component of the magnetic field are also expressed on the surface R_0 (Eqs 18, 19, 20, 21), so we are facing a problem where V_1^* and V_2^* are known on boundaries respectively R_i and R_s, and are equal on R_0. The difference of their gradient with respect to r coordinate are also known on R_0 . We are then facing a Dirichlet problem when considering region one and two together. Solutions of such a problem are unique.

Almost similar arguments can be followed in the looking for the vector potential. Current densities are present on R_i and R_0. The rotor and the stator still have infinite permeability, the interior of the azimuth magnets being empty space. The jump of the tangential component of the flux density on R_i gives a value to the gradient of the vector potential with respect to r coordinate on that boundary (Eqs 18, 19, 20, 21). That gradient is zero on the interior surface of the stator, because only the flux density due to the azimuth magnets is looking for. So, no current is assumed on the stator. We are then facing here a Neuman problem when considering region one and two together. Solutions of such a problem are also unique.

The operation of derivation is linear, so usually solutions of those Dirichlet and Neuman problems can be a sum of harmonics. We can then write $V_1^* = \sum_{n=1}^{n=\infty} V_{1n}^*$, $V_2^* = \sum_{n=1}^{n=\infty} V_{2n}^*$, $A_1 = \sum_{n=1}^{n=\infty} A_{1n}$, and $A_2 = \sum_{n=1}^{n=\infty} A_{2n}$, where V_1^*, V_2^*, A_1, and A_2, are respectively the total magnetic scalar potential in region one, in region two, the total vector potential in region one and in region two. V_{1n}^*, V_{2n}^*, A_{1n}, and A_{2n} are the corresponding harmonics, on which Laplace's equation is applied. According to the method of the separation of variables, each of these functions is a product of a function of r and a function of θ. The structures are cylindrical, given the Fourier's development of the sources in cos $\nu\theta$, the solutions will have the forms r^{ν} cos $\nu\theta$, and $r^{-\nu}$ cos $\nu\theta$, which can be expressed with respect to R_0, (Eqs 14, 15, 16, 17).Coefficients, c_n, d_n, f_n, g_n, α_n, β_n, δ_n, and γ_n are then determined owing to the boundaries conditions (Eqs 18, 19, 20, 21, 23, 25).

Since both cylinders of radii R_i and R_0 carry charge density and current density, we can then write :

$$V_1^* = \sum_{n=0}^{\infty} \left[c_n \left(\frac{r}{R_o} \right)^{\nu} + d_n \left(\frac{R_o}{r} \right)^{\nu} \right] \sin \nu\theta \tag{14}$$

$$V_2^* = \sum_{n=0}^{\infty} \left[f_n \left(\frac{r}{R_o} \right)^{\nu} + g_n \left(\frac{R_o}{r} \right)^{\nu} \right] \sin \nu\theta \tag{15}$$

$$A_1 = \sum_{n=0}^{\infty} \left[\alpha_n \left(\frac{r}{R_o} \right)^{\nu} + \beta_n \left(\frac{R_o}{r} \right)^{\nu} \right] \cos \nu\theta \tag{16}$$

$$A_2 = \sum_{n=0}^{\infty} \left[\gamma_n \left(\frac{r}{R_o} \right)^{\nu} + \delta_n \left(\frac{R_o}{r} \right)^{\nu} \right] \cos \nu\theta \tag{17}$$

with the following boundary conditions :

for $r = R_i$

$$V_1^* = 0 \qquad \frac{\partial A_1}{\partial r} = -\mu_o K(R_i, \theta) \tag{18}$$

for $r = R_o$

$$V_1^* = V_2^* \qquad A_1 = A_2 \tag{19}$$

or

$$\frac{\partial A_2}{\partial r} - \frac{\partial A_1}{\partial r} = -\mu_o K(R_o, \theta)$$

$$\frac{\partial V_2^*}{\partial r} - \frac{\partial V_1^*}{\partial r} = -\sigma^*(R_o, \theta) \tag{20}$$

for $r = R_s$

$$V_2^* = 0 \qquad \frac{\partial A_2}{\partial r} = 0 \tag{21}$$

3.1.2. Analytical expressions of the flux density with respect to magnets properties

Exploiting the above boundary conditions we have the following relations between the coefficients :

On one hand, putting $s_a = \mu_o R_o K_o a_n / \nu$, it is obtained :

$$\begin{aligned} &\left(\frac{R_i}{R_o}\right)^{\nu} \alpha_n - \left(\frac{R_o}{R_i}\right)^{\nu} \beta_n = S_a \\ &\alpha_n + \beta_n - \gamma_n - \delta_n = 0 \\ &\alpha_n - \beta_n - \gamma_n + \delta_n = S_a \\ &\left(\frac{R_s}{R_o}\right)^{\nu} \gamma_n - \left(\frac{R_o}{R_s}\right)^{\nu} \delta_n = 0 \end{aligned} \qquad (22)$$

which lead to the following solutions :

$$\begin{aligned} \gamma_n &= \frac{\left[1 - \left(\frac{R_i}{R_o}\right)^{2\nu}\right]\left(\frac{S_a}{2}\right)}{\left(\frac{R_s}{R_o}\right)^{2\nu} - \left(\frac{R_i}{R_o}\right)^{2\nu}} \\ \delta_n &= \left(\frac{R_s}{R_o}\right)^{2\nu} \gamma_n \\ \alpha_n &= \gamma_n + \left(\frac{S_a}{2}\right) \\ \beta_n &= \left(\frac{R_s}{R_o}\right)^{2\nu} \gamma_n - \left(\frac{S_a}{2}\right) \end{aligned} \qquad (23)$$

On the other hand, with $s_b = \sigma_o^* R_o b_n / \nu$, it is obtained :

$$\begin{aligned} &\left(\frac{R_i}{R_o}\right)^{\nu} c_n - \left(\frac{R_o}{R_i}\right)^{\nu} d_n = 0 \\ &c_n + d_n - f_n - g_n = 0 \\ &c_n - d_n - f_n + g_n = S_b \\ &\left(\frac{R_s}{R_o}\right)^{\nu} f_n - \left(\frac{R_o}{R_s}\right)^{\nu} g_n = 0 \end{aligned} \qquad (24)$$

which gives the solutions :

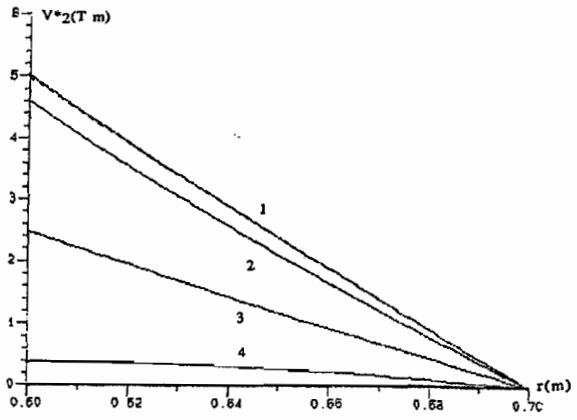

Fig.3 Magnetic scalar potential V_2^* (T m) varying as a function of r(m) radial coordinates centered on radial magnets. Azimuth magnets have not been used. The study has been performed here in two and three dimensions.

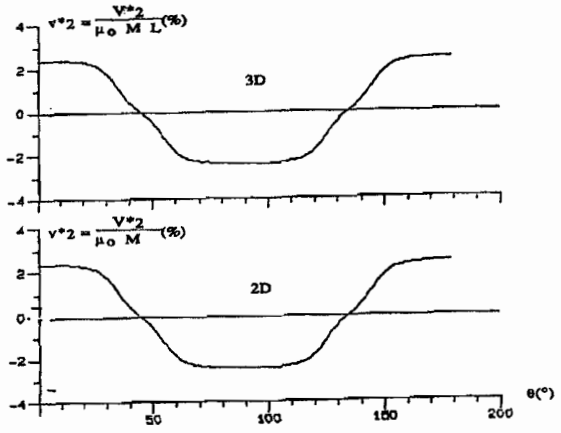

Fig.4 Reduced magnetic scalar potential v_2^* (%) varying as a function of q (°) tangential coordinates.

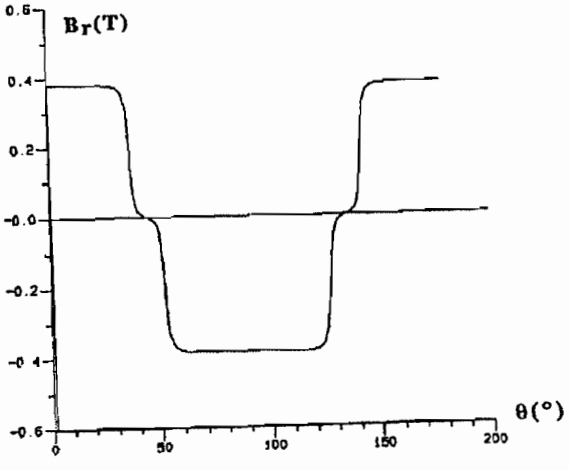

Fig.5 Radial flux density in the air-gap calculated by the method of the separation of variables.

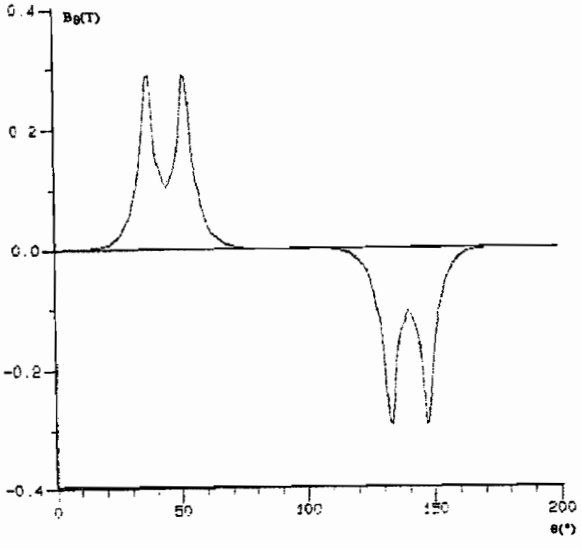

Fig.6 Tangential flux density in the air-gap calculated by the method of the separation of variables.

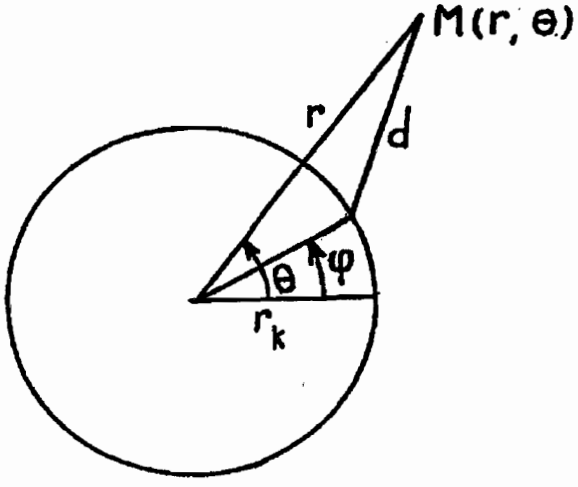

Fig.7 k image cylinder and point M(r, q) in the air gap

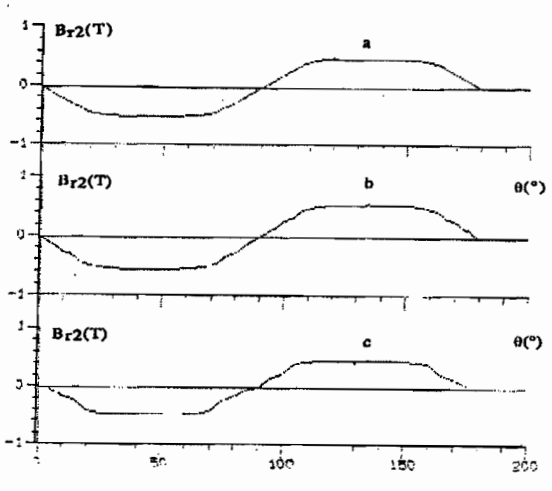

Fig.8 Radial flux density

$$f_n = \frac{\left[1 - \left(\frac{R_i}{R_o}\right)^{2\nu}\right]\left(\frac{S_b}{2}\right)}{\left(\frac{R_i}{R_o}\right)^{2\nu} - \left(\frac{R_s}{R_o}\right)^{2\nu}}$$

$$g_n = -\left(\frac{R_s}{R_o}\right)^{2\nu} f_n \qquad (25)$$

$$c_n = f_n + \left(\frac{S_b}{2}\right)$$

$$d_n = -\left(\frac{R_s}{R_o}\right)^{2\nu} f_n - \left(\frac{S_b}{2}\right)$$

Fig.3 Magnetic scalar potential V_2*(T m) varying as a function of r(m) radial coordinates centered on radial magnets. Azimuth magnets have not been used. The study has been performed here in two and three dimensions.
Machine Data : $R_s = 0.7$ m $R_o = 0.6$ m $R_i = 0.5$ m. $p = 2$
$2\theta_{ra} = 75°$ $\theta_{az} = 0°$ $\theta_{is} = 0°$
$l_m = 0.5$ m $L_m = 0.8$ m $\mu_o M = 0.92$ T (NdFeB)
Studied points : $\theta = 0°$ (1) $z = 0$ (2) $z = 0.4$ m
(3) $z = 0.5$ m (4) $z = 0.6$ m

Fig.4 Reduced magnetic scalar potential v_2*(%) varying as a function of θ (°) tangential coordinates. Azimuth magnets have not been used. The study has been performed here in two and three dimensions.
*** In two dimensions (2D)**
Machine Data: $R_s = 0.7$ m $R_o = 0.6$ m $R_i = 0.5$ m. $p = 2$
$2\theta_{ra} = 75°$ $\theta_{az} = 0°$ $\theta_{is} = 0°$
Studied points : $r = 0.65$ m

*** In three dimensions (3D)**
Machine Data: $R_s/L = 87.5\%$ $R_i/L = 62.5\%$ $R_o/L = 75\%$ $p = 2$
$2\theta_{ra} = 75°$ $\theta_{az} = 0°$ $\theta_{is} = 0°$
Studied points : $r/L = 81.25\%$ $l_m / L_m = 62.5\%$

As seen above, the only component of $\vec{B}$ needed for the torque calculation is B_r in region 2. We have from Eq.13 the following expressions :

$$B_{r2}(r,\theta) = -\left(\frac{\mu_o \nu}{r}\right)\sum_{n=0}^{\infty}\left[\left(\gamma_n + f_n\right)\left(\frac{r}{R_o}\right)^{\nu} + \left(\delta_n - g_n\right)\left(\frac{R_o}{r}\right)^{\nu}\right]\sin \nu\theta \qquad (26)$$

$$B_{\theta 2}(r,\theta) = \frac{1}{r}\sum_{n=0}^{\infty}\nu\left[\left(f_n - \gamma_n\right)\left(\frac{r}{R_o}\right)^{\nu} + \left(\delta_n + g_n\right)\left(\frac{R_o}{r}\right)^{\nu}\right]\cos \nu\theta$$

Fig.5 Radial flux density in the air-gap calculated by the method of the separation of variables.
Studied points : r=7.38 cm.

Machine Data : R_s = 8.39 cm R_o=7.23 cm R_i=6.48 cm. p = 2
$2\theta_{ra}$= 75° θ_{az}= 0° θ_{is}= 0°
$\mu_o M$ = 0.92 T (NdFeB)

Fig.6 Tangential flux density in the air-gap calculated by the method of the separation of variables.
Studied points : r=7.38 cm.
Machine Data : R_s = 8.39 cm R_o=7.23 cm R_i=6.48 cm. p = 2
$2\theta_{ra}$= 75° θ_{az}= 0° θ_{is}= 0°
$\mu_o M$ = 0.92 T (NdFeB)

3.2. AN OTHER ORIGINAL ANALYTICAL METHODOLOGY BASED ON MAGNETIC IMAGES AND TCHEBYCHEV'S POLYNOMIALS

In the method of magnetic images, all iron parts are removed and replaced by air in which the images of the original sources will be located. We have then determined the values of these image sources and their positions.

Because magnetic permeabilities are infinite, the image of a charged line with a density λ^* is a line with a density $-\lambda^*$ and the image of a current line with a density J^* is a line with a density $-J^*$.

The position of the image of a line (of charge or current) with respect to a magnetic cylinder of radius R is such that

$$d\,D = R^2 \tag{27}$$

where d and D are the distances of the line and its image to the axis. Consequently, it can be seen that we have to consider both magnet surfaces as regards current densities and only the external one as regards charge densities (Fig.1b).

In the present case, the sources are included between two concentric ferromagnetic domains, thus they generate an infinity of images, the positions of which have to be determined.

3.2.1.Calculation of the positions of images.

From equation (27), putting :

$$\rho = R_i^2/R_s^2 \tag{28}$$

we get the radial positions $r_k < R_i$ of the inner images and $R_k > R_s$ of the outer images as the following sequences :

for the original surface $r = R_o$

$$\begin{array}{llll} r_o = R_o & r_1 = \dfrac{R_i^2}{r_o} & r_{2k} = r_o \rho^k & r_{2k+1} = r_1 \rho^k \\ R_o & R_1 = \dfrac{R_s^2}{R_o} & R_{2k} = R_o \rho^{-k} & R_{2k+1} = R_1 \rho^{-k} \end{array} \tag{28}$$

and for the original surface $r = R_i$

$$\begin{array}{llll} r'_o = R_i & r'_1 = \dfrac{R_i^2}{r'_o} & r'_{2k} = r'_o \rho^k & r'_{2k+1} = r'_1 \rho^k \\ R'_o = R_i & R'_1 = \dfrac{R_s^2}{R'_o} & R'_{2k} = R'_o \rho^{-k} & R'_{2k+1} = R'_1 \rho^{-k} \end{array} \tag{29}$$

3.2.2.Calculation of the radial flux density.

We can now calculate the total scalar and vector potentials and deduce the radial component of the flux density.

We first calculate the potentials V_k^* and A_k due to k^{th} image surface then sum for all the images.

In the domain 2, we have :

$$B_{r2}(r,\theta) = -\mu_o \frac{\partial V_2^*}{\partial r} + \frac{1}{r}\frac{\partial A_2}{\partial \theta} \tag{30}$$

and according to figure 3

$$V_2^* = \sum_{k=o}^{\infty} V_k^* \qquad A_2 = \sum_{k=o}^{\infty} A_k \qquad \text{with} \qquad V_k^* = \frac{(-1)^k \sigma_o^* R_o}{4\pi} \sum_{n=o}^{\infty} b_n I \tag{31}$$

and $$A_k = \mu_o \frac{K_o R_o}{4\pi} \sum_{n=o}^{\infty} a_n (J + J')$$

$$I = \int_o^{2\pi} \ln d^2 \sin \nu\varphi \, d\varphi \qquad J = \int_o^{2\pi} \ln d^2 \cos \nu\varphi \, d\varphi \qquad J' = \int_o^{2\pi} \ln d'^2 \cos \nu\varphi \, d\varphi \tag{32}$$

with :

$$d^2 = r^2 + r_k^2 - 2 r r_k \cos(\theta - \varphi) \qquad d'^2 = r^2 + r_k'^2 - 2 r r_k' \cos(\theta - \varphi) \tag{33}$$

V_k^* and A_k are generated respectively by image surfaces carrying charge densities and current densities (Fig.7). They are due to respectively the four and eight surfaces defined by their radii of subscripts 2k and 2k + 1 (Eqs.28 to 29).

Integrating by parts (32), we get the following integrals :

$$I = \int_o^{2\pi} \frac{\cos \nu\varphi}{d^2} d\varphi \qquad \text{and} \qquad J = \int_o^{2\pi} \frac{\sin \nu\varphi}{d^2} d\varphi \tag{34}$$

For diverse reasons, approximation is achieved using Tchebychev's polynomials [7].

So setting $\Psi = \varphi - \theta$, we obtain :

$$\frac{1}{d} \approx \sum_{\ell=o}^{X} b_\ell \cos \ell\Psi \tag{35}$$

where

$$b_\ell = \frac{2}{X+1} \sum_{i=o}^{i=X} \frac{1}{d^2(\Psi_i)} \cos \ell\Psi_i \tag{36}$$

$$\Psi_i = \left(\frac{2i+1}{X+1}\right)\frac{\pi}{2}$$

Ψ_i is the i^{th} point of Tchebychev's interpolation

So :

$$I = \pi b_\nu \cos \nu\theta$$
$$J = \pi b_\nu \sin \nu\theta \tag{37}$$

Obviously the expressions involving d' are similar. So, putting :

$$\beta_\nu = \frac{b_{\nu-1} - b_{\nu+1}}{\nu}$$
$$\beta'_\nu = \frac{b'_{\nu-1} - b'_{\nu+1}}{\nu} \tag{38}$$

and remembering that $\nu = (2n + 1)p$, we have :

$$V_k^* = \frac{(-1)^k \sigma_o^* R_o}{4} r r_k \sum_{n=o}^{\infty} b_n \beta_\nu \sin \nu\theta \tag{39}$$

$$A_k = -\mu_o \frac{K_o R_o}{4} r r_k \sum_{km=o}^{\infty} a_n \beta_\nu \cos \nu\theta \; - \; \mu_o \frac{K_o' R_o'}{4} r r_k' \sum_{km=o}^{\infty} a_n \beta'_\nu \cos \nu\theta \tag{40}$$

and finally :

$$B_{r2}(r,\theta) = \mu_o \frac{\sigma_o^* R_o}{4} \sum_{k=o}^{\infty} (-1)^k r_k \sum_{n=o}^{\infty} b_n \beta_\nu \sin \nu\theta$$

$$+ \quad \mu_o \frac{\sigma_o^* R_o}{4} r \sum_{k=o}^{\infty} (-1)^k r_k \sum_{n=o}^{\infty} b_n \left(\frac{\partial \beta_\nu}{\partial r} \right) \sin \nu\theta \qquad (41)$$

$$+ \quad \mu_o \frac{K_o R_o}{4} \sum_{k=o}^{\infty} r_k \sum_{n=o}^{\infty} a_n \beta_\nu \sin \nu\theta$$

$$+ \quad \mu_o \frac{K_o' R_o'}{4} \sum_{k=o}^{\infty} r_k' \sum_{n=o}^{\infty} a_n \beta_\nu' \sin \nu\theta$$

Fig.8 Radial flux density calculated by
- the separation of variables (a),
- the method of magnetic images with 5 images (b),
-the numerical method (c).

Studied points : r=0.65m.

Machine Data : $R_s = 0.7$m R_o=0.6m R_i=0.5m p = 2

θ_{ra}=30° θ_{az}=10° θ_{is}=5°.

$\mu_o M = 0.92$ T (NdFeB)

3.3. CALCULATIONS OF THE MAGNETIC FIELD LINES AND OF THE FLUX DENSITY USING A FINITE DIFFERENCE PROGRAM CALLED "DIFIMEDI"

The finite difference program "DIFIMEDI" [9] has been used in order to compare the numerical results to those obtained from the models presented in the above sections. For similar accuracy, computing times are compared too.

As seen in Fig.9, only half a machine has been considered. The permeabilities respectively have the values 1 for the magnets and the air gap, and 1000 for the iron parts.

The number of nodes in DIFIMEDI is 25x37.

Fig.9 Flux density lines due to permanent magnets with radial (R) and azimuth (A) magnetizations.
Machine Data : $R_s = 0.7$m R_o=0.6m R_i=0.5m
θ_{ra}=30° θ_{az}=10° θ_{is}=5°.

4. RESULTS

The radial component due to the magnets is calculated in the air gap or along the stator. Both analytical models lead to the same results in all cases, and the maximum difference observed between these results and numerical ones obtained by F.D.M is less than 7 %.

In practice, terms of rank higher than 4 have no significant influence on the results obtained by means of separation of variables. The same accuracy is obtained with only five images in the second analytical method.

The computing times, excluding parameter inputs, for calculating the flux density are :
- 4 seconds for the separation of variables.
- 6 seconds for the magnetic image method.
- 12 seconds for the finite differences method (Fig.8, 9).

Obviously, variations of geometrical parameters or positions of the rotor are more easily implemented in the analytical methods. Besides, the computation time when using the finite differences method takes into account the calculation of the flux density at every node, which is of no use in the calculation of the torque. Both analytical studies show that azimuth magnets must be used to get more sinusoidal flux densities in synchronous machines (Fig.5). If the machines are used as brush-less DC motors, the flux density can be chosen trapezoidal and the best way is to use only radial magnets filling the whole slot (Fig.6, 10).

Assuming the machine fed by rectangular currents, and for given dimensions of the magnets, the effect of the azimuth ones on the torque is notable (Fig.14). When stator conductors are located in the slots, the torque is smaller for given located currents and number of conductors per pole per phase (Fig.15).

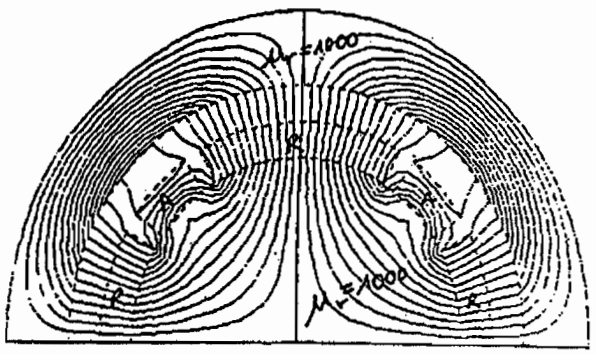

Fig.9 Flux density lines due to permanent magnets with radial (R) and azimuth (A) magnetizations.

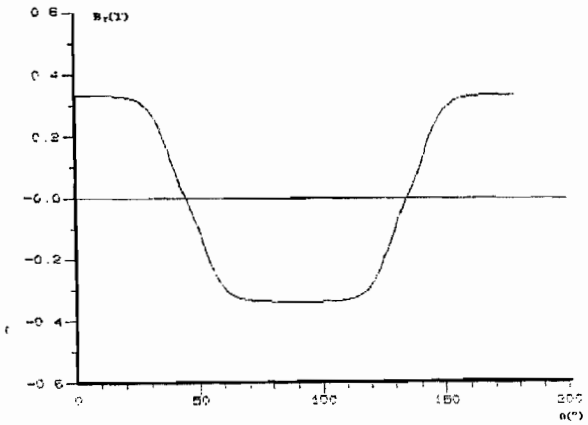

Fig.10 Radial flux density on the interior surface of the stator calculated by the method of the separation of variables.

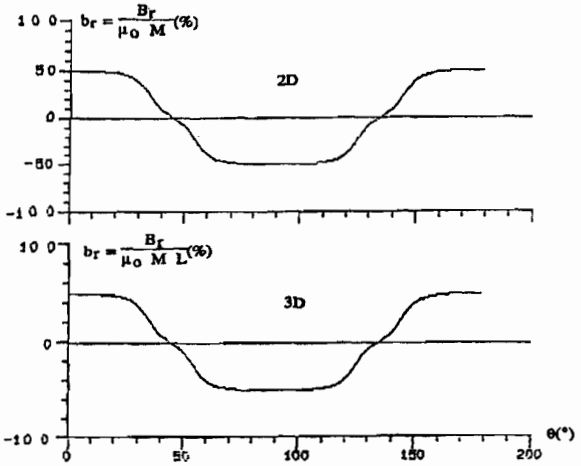

Fig.11 Reduced radial flux density b_r^*(%) varying as a function of q (°) tangential coordinates.

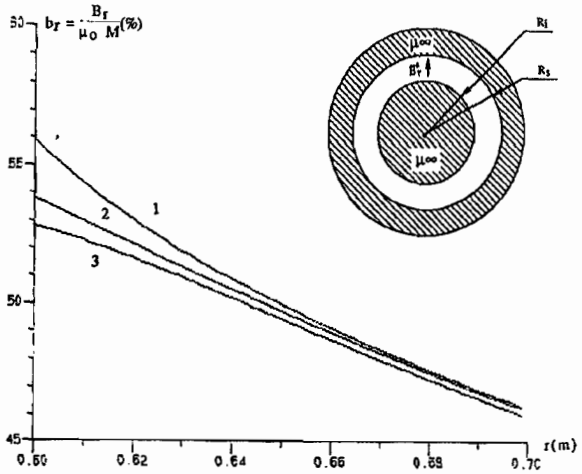

Fig.12 Reduced radial flux density b_r^*(%) varying as a function of r (m) radial coordinates centered on radial magnets

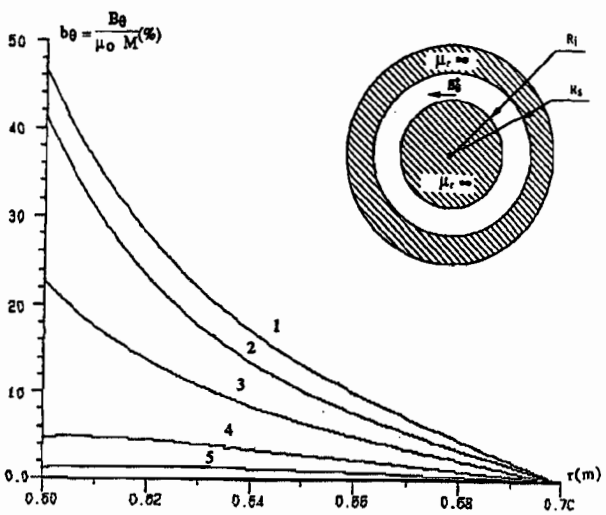

Fig.13 Reduced tangential flux density bq^*(%) varying as a function of r (m) radial coordinates centered on radial magnets.

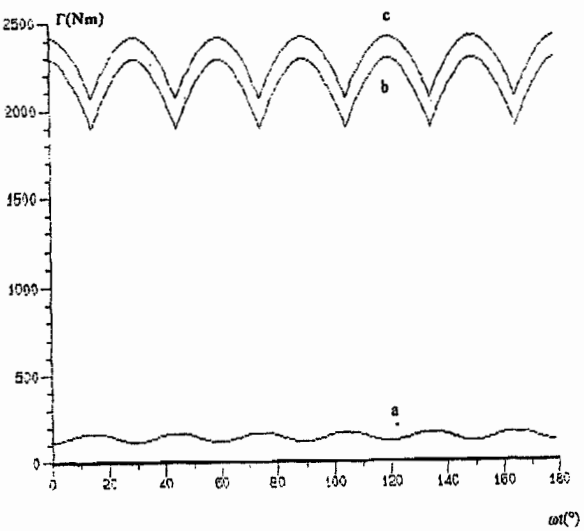

Fig.14 Instantaneous torques for rectangular currents in slot less machines.

Fig.10 Radial flux density on the interior surface of the stator calculated by the method of the separation of variables.
Studied points : r=8.39 cm.
Machine Data : R_s = 8.39 cm R_o=7.23 cm R_i=6.48 cm. p = 2
$2\theta_{ra}$= 75° θ_{az}= 0° θ_{is}= 0°
$\mu_o M$ = 0.92 T (NdFeB)

Fig.11 Reduced radial flux density b_r*(%) varying as a function of θ (°) tangential coordinates. Azimuth magnets have not been used. The study has been performed here in two and three dimensions.
*** In two dimensions (2D)**
Machine Data: R_s = 0.7 m R_o = 0.6 m R_i = 0.5 m. p = 2
$2\theta_{ra}$= 75° θ_{az}= 0° θ_{is}= 0°
Studied points : r = 0.65 m

*** In three dimensions (3D)**
Machine Data: R_s /L = 87.5 % R_i /L = 62.5 % R_o /L = 75 % p = 2
$2\theta_{ra}$= 75° θ_{az}= 0° θ_{is}= 0°
Studied points : r /L = 81.25 % l_m / L_m = 62.5 %

Fig.12 Reduced radial flux density b_r*(%) varying as a function of r (m) radial coordinates centered on radial magnets. Azimuth magnets have not been used. The study has been performed here in two and three dimensions.
*** In two dimensions (2D)**
Machine Data: R_s = 0.7 m R_o = 0.6 m R_i = 0.5 m. p = 2
$2\theta_{ra}$= 75° θ_{az}= 0° θ_{is}= 0°
Studied points : (1) θ = 0°

*** In three dimensions (3D)**
Machine Data: R_s = 0.7 m R_o = 0.6 m R_i = 0.5 m. p = 2
$2\theta_{ra}$= 75° θ_{az}= 0° θ_{is}= 0° l_m= 0.5 m L_m= 0.8 m
Studied points : (2) θ = 0° ; z = 0.1 m (3) θ = 0° ; z = 0.2 m

Fig.13 Reduced tangential flux density b_θ*(%) varying as a function of r (m) radial coordinates centered on radial magnets. Azimuth magnets have not been used. The study has been performed here in two and three dimensions.
*** In two dimensions (2D)**
Machine Data: R_s = 0.7 m R_o = 0.6 m R_i = 0.5 m. p = 2
$2\theta_{ra}$= 75° θ_{az}= 0° θ_{is}= 0°
Studied points : (1) θ = 35°

*** In three dimensions (3D)**
Machine Data: R_s = 0.7 m R_o = 0.6 m R_i = 0.5 m. p = 2
$2\theta_{ra}$= 75° θ_{az}= 0° θ_{is}= 0° l_m= 0.5 m L_m= 0.8 m
Studied points : (2) θ = 35° ; z = 0.45 m (3) θ = 35° ; z = 0.5 m
(4) θ = 35° ; z = 0.55 m (5) θ = 35° ; z = 0.6 m

Fig.14 Instantaneous torques for rectangular currents in slot less machines. The radial flux density has been calculated by the separation of variables. Case of constant density of phase conductors.
Studied points : r=0.7m.
Machine Data : R_s = 0.8m R_o=0.6m R_i=0.5m. p = 2 $\mu_o M$ = 0.92 T (NdFeB)
Parameters : θ_{ra}, θ_{az} and θ_{is}
a) Torque due to only azimuth magnets.
(θ_{ra}=0° θ_{az}=10° θ_{is}=0°).
b) Torque due to only radial magnets.
(θ_{ra}=30° θ_{az}=0° θ_{is}=0°).
c) Torque due to both radial and azimuth magnets.
(θ_{ra}=30° θ_{az}=10° θ_{is}=5°).

Fig.15 Instantaneous torques for rectangular currents in slot less machines. The radial flux density has been calculated by the separation of variables. Case of none constant density of phase conductors.
Studied points : r=0.7m.

Machine Data : $R_s = 0.8m$ $R_o=0.6m$ $R_i=0.5m.$ $p = 2$ $\mu_o M = 0.92$ T (NdFeB)
$\theta_{ra}=35°\theta_{az}=10°$ $\theta_{is}=0°$

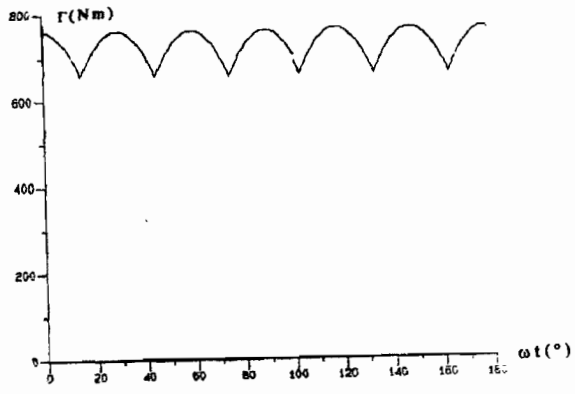

CONCLUSION

An analytical study of a given structure of permanent magnets synchronous machine has been achieved, and numerically verified. After finding out suitable original models of the magnets made by equivalent surfaces of charges and currents, an original analytical study has been done using the classic variable separation method, and an interesting application of the method of magnetic images, in cylindrical domains. The comparison of a finite difference program show a close agreement.

Both analytical methods present, in comparison with numerical ones, considerable advantages as mentioned in [9] which are :

- the rapidity.
- the easiness of the definition and modification of the geometry.
- the high accuracy of the analytical methods.
- the reasonable size of memory (a personal computer is sufficient).
- the possibilities of exploiting the results, for instance, the study of the influence of each parameter independently.
- the pre-dimensioning of the motors
- the optimization of the motors

The analysis of the results shows the interest of the azimuth magnets on the form of the flux density and the value of the torque. An extension of the present work can be a detailed study of the effects of radial and azimuth permanent magnets on the torque (average value and harmonics). Another application could be the examination of the azimuth width of magnets in order to adapt converters to such machines.

ACKNOWLEDGEMENTS

The authors thank Pr.Bernard DAVAT, Pr.Bernard LAPORTE, the memory of Pr.Edmond Jules GUDEFIN, Pr.Shahrokh SAADATE, and Pr.Tabar MEIBODY for their helpful discussions. Theoretical results have been drawn out using the software « DSN » from LEEI-Laboratory (TOULOUSE). The authors would also like to address grateful thanks to the University of Ngaoundéré in Cameroun, through its GPRU ("Grand Projet de recherches : Genie Industriel; Projet : Conception et Réalisation de Dispositifs de Transformation d'Energie Electrique").

REFERENCES

[1] J.DHERS, R.G.E.-Journal, N°3, March (1987).
[2] G.R.POLGREEN, *New Applications of Modern Magnets*, edited by Mac Donald, London (1966).
[3] M.K.JENKINS, D.HOWE, *Proceedings of European Symposium, GRENOBLE, 1990,* edited by IEG-LEG-URA CNRS 355, part 5, pp.1-8.
[4] N.GUILBERT, *Proceedings of European Symposium, GRENOBLE, 1990,* edited by IEG-LEG-URA CNRS 355, part 3, pp1-7.
[5] M.LAJOIE-MAZENC, P.MATHIEU, B.DAVAT, R.G.E.-Journal, N°10, October (1984).
[6] A.REZZOUG, Ph.D.thesis, Polytechnic National Institute of Lorraine (INPL), Nancy, France, (1987).
[7] F.M.SARGOS, A.REZZOUG, M.T.ATTAF, Revue Of Applied Physics, N°23, August, (1988).
[8] A.YOUMSSI, A.REZZOUG, F.M.SARGOS, E.J.GUDEFIN, The European Physical Journal (EPJ-Applied Physics) Vol 8, Number 2, November 1999, pp 163-170.
[9] Polytechnic National Institute of Toulouse (France), « Laboratoire d'Electrotechnique et d'Electronique Industrielle de l'ENSEEIHT, CNRS – URA 847, 2 rue camichel, 31071 Toulouse, France », Finite differences code called : DIFIMEDI, 1990.
[10] J.L. COULOMB, J.C. SABONNADIERE, *CAO En Electrotechnique* (Hermes Publishing, Paris, 1985). Chapter1 and 2.